SEMI-ANNUAL TECHNICAL REPORT

TECHNOLOGY FOR SATELLITE POWER CONVERSION

Prepared by

M. A. Gouker, D. P. Campbell and J. J. Gallagher

Prepared for

NATIONAL AERONAUTICS AND SPACE ADMINISTRATION
Lewis Research Center
21000 Brookpark Road
Cleveland, Ohio 44135

Under

NASA Research Grant No. NAG3-282

and

Georgia Tech Research Institute Project No. 3244

NASA Technical Officer: W. M. Krawczonek

January 29, 1986

GEORGIA INSTITUTE OF TECHNOLOGY
A Unit of the University System of Georgia
Atlanta, Georgia 30332

GTRI
GEORGIA TECH RESEARCH INSTITUTE

1986

Semi-Annual Technical Report
on
Technology for
Satellite Power Conversion

NASA Research Grant
No. NAG3-282
Georgia Tech Research Institute
Project No. 3244

NASA Technical Officer: W. M. Krawczonek

Prepared for

National Aeronautics and Space Administration
Lewis Research Center
21000 Brookpark Road
Cleveland, Ohio 44135

Prepared by

M. A. Gouker
D. P. Campbell
J. J. Gallagher

Georgia Tech Research Institute
Georgia Institute of Technology
Atlanta, Georgia 30332

January 29, 1986

Table of Contents

1. INTRODUCTION

During the past reporting period, investigations have been concerned mainly with the measurement of the pattern of the dipole antennas at 230 GHz. Previous measurements have shown antenna effects, but these have been combined with effects from currents induced in the bonding wires flowing through the bolometer. New designs, discussed in the text, have resulted in improved detection from the antenna configuration. This improvement will aid in the rectification schemes. In performing these antenna investigations, improvements have resulted in measurement techniques for precise antenna pattern observations. Fabrication of the MOM diode has been started and is discussed for work during the next period.

2. SUMMARY OF WORK COMPLETED

During the six month period of this report (23 April, 1985 through 28 October, 1985) the dipole pattern of the antenna has been confirmed and work on the MOM diode has begun. The antenna - detector structure was modified and the measurement apparatus reconfigured to permit precise antenna pattern measurements. Fabrication of the MOM diode was initiated after antenna action from the new structures was observed.

The major effort in this period was the development of a refined antenna structure. The previous antenna design allowed currents induced by the incident radiation in the bonding wires to flow through the bolometer. The detector was thus responding to both the antenna and bonding wire currents. A low pass filter was added to the antenna structure to improve the detection scheme. The new design uses an interdigitated capacitor to prevent the induced current in the bonding wires from flowing

through the detection element. The original antenna design as well as newly published calculations [1] are included in the new structure. The resultant design consists of a dipole antenna 10 X 390 μm and transmission lines 10 μm wide. Full details are given in Sections 3 and 4.

A micropositioner which facilitates precise antenna pattern measurements was also designed and fabricated in this reporting period. This structure and other refinements to the measurement apparatus are described in Section 5.

Section 6 contains the new antenna patterns and a preliminary test of a beam lead diode bonded to an old antenna. Conclusions and future work on the MOM diode are discussed in Section 7.

3. ANTENNA DESIGN

A new antenna structure using an interdigitated capacitor has been developed to facilitate antenna pattern measurements. The previous design, shown in Figure 1, contained the dipole antenna and a quarter wavelength transmission line terminating to the bismuth bolometer. Bonding pads just beyond the bolometer allow connection of the antenna with the external bias/detection circuit. It was determined that this arrangement allowed currents induced in the bonding wires to flow freely through the bolometer, thereby masking the true pattern of the antenna.

A straightforward refinement to the design was to fabricate a low pass filter between the bonding wires and the bolometer. The 230 GHz signal induced in the bonding wires is thus prevented from reaching the bolometer and the low frequency signal for the lock in amplifier detection circuit is not effected.

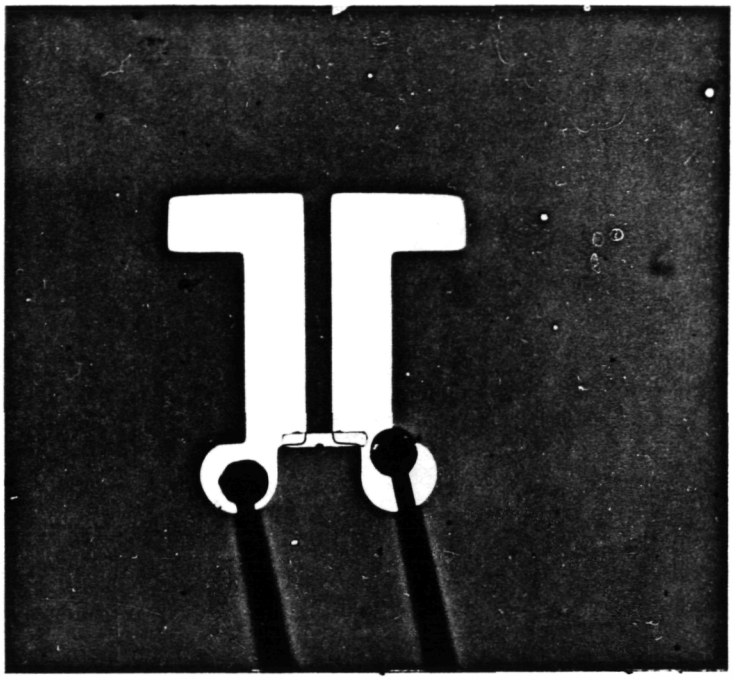

Figure 1. Previous antenna design with transmission lines, Bismuth bolometer and bonding pads. Currents induced in the bonding wires from the incident field are free to flow through the bolometer, thereby masking the true pattern of the antenna.

The new design* shown in Figure 2, consists of dipole antenna with a horseshoe shaped bolometer at the terminals of the antenna and transmission lines. The thinner width of the dipole is consistent with existing models for antennas on substrates where the current is assumed to flow in one dimension parallel with the axis of the dipole. The six-finger interdigitated capacitor has a calculated capacitance of 0.2 pF. The transmission line was made as long as experimental procedure would permit to keep the bonding wires at a reasonable distance from the antenna. Each of the substructures is discussed in detail below.

3.1 Antenna Parameters

The antenna design parameters are from a recent publication by Kominami et al [1]. The ratio of width to length of the antenna is assumed to be 0.02 and the antenna is taken to lie on a dielectric half-space, i.e. the substrate is infinitely thick. The issue of substrates with finite thicknesses greater than several wavelengths has not been addressed in this or other work in the literature. The design parameters in [1] were used for the finite substrate without modification.

A resonant length of an antenna is by definition any given length which makes the radiation resistance of the dipole purely real and finite. For an antenna on a substrate both the resonant length and corresponding resonant resistance are a function of the dielectric constant. In free space the purely real

---

* Dr. Glenn Smith, Professor in the school of Electrical Engineering and coauthor of Antennas in Matter by MIT Press, has assisted with the antenna design.

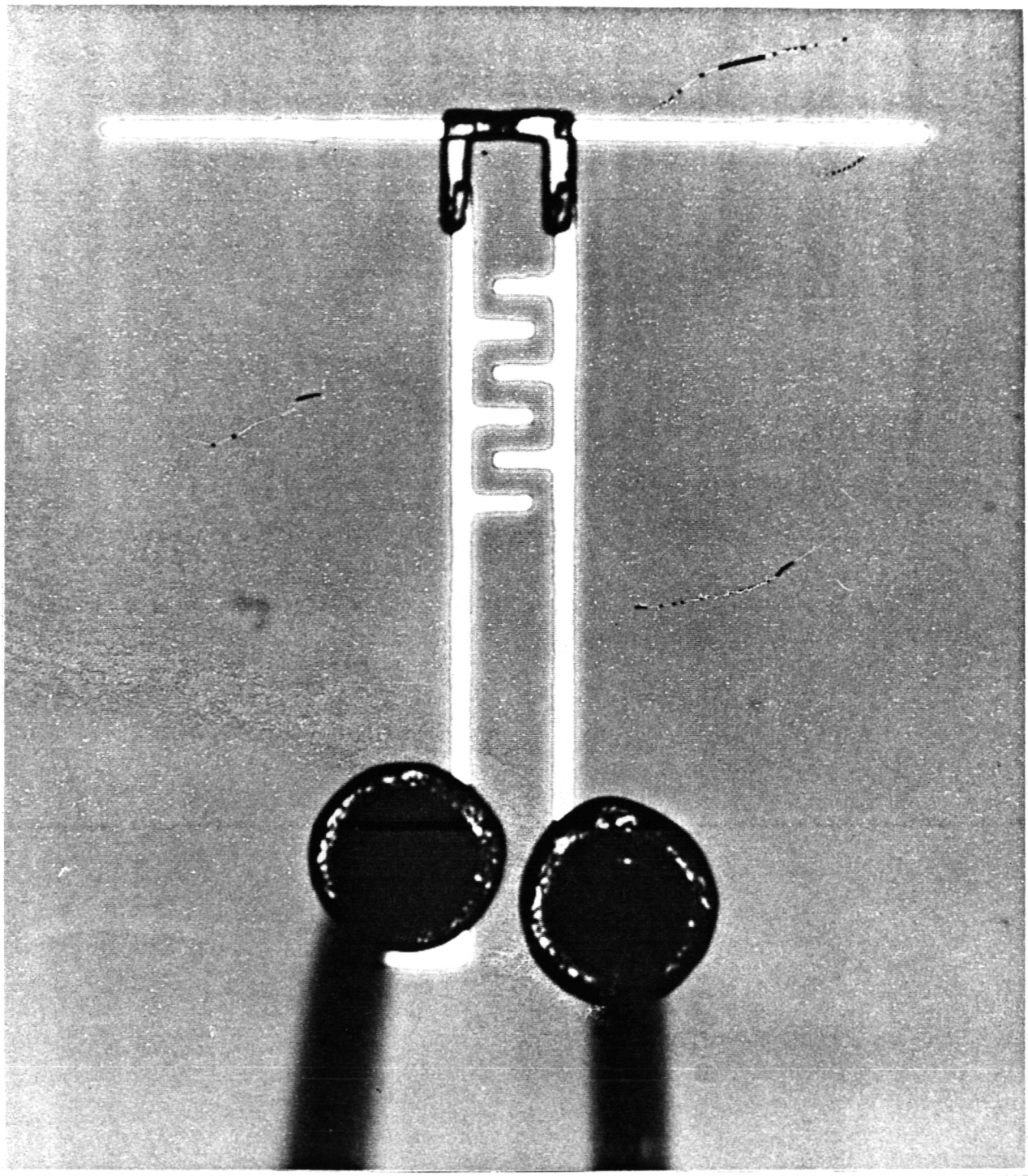

Figure 2. New antenna design with horseshoe shaped bolometer, interdigitated capacitor, transmission line and bonding pads. The antenna is 390 microns long, and all structures are 10 microns wide.

resistance of 73 Ω corresponds to a resonant length of one- half wavelength. The values for an antenna on a dielectric half-space are between the values for a free space antenna and those for a dipole embedded in the dielectric. The resonant length is given to a good approximation by

$$\frac{L}{\lambda_o} = \frac{1}{\sqrt{\epsilon_e}} \, 0.48 \, \frac{1}{1 + W/L}$$

where $\epsilon_e = (1 + \epsilon_r)/2$ and W/L is the width-to-length ratio of the dipole. The corresponding resonant resistance is found from plots given in [1]. For a relative dielectric constant of 4, the resonant length is 0.3 λ o (390μm for λo = 1.3mm) and the resonant resistance is 55Ω .

3.2 Transmission Line and Bolometer

The impedance of the antenna and that of the load (either the bolometer or the rectifying diode) must be matched in order for the antenna to deliver all received power to the load. If the resistance of the bolometer is taken to be purely real, i.e. no parasitic capacitance in the Au-Bi junction is assumed, a transmission line to match the antenna and the load is not required. A bolometer with resistance equal to the resonant resistance of the antenna is placed at the terminals of the antenna for maximum power transfer. If, however, the load is a rectifying diode, there is limited freedom associated with the impedance of the device. A matching transmission line must then be used to optimize the rectified current.

3.3 Low Pass Filter

Introduction of a low pass filter prevents the current induced in the bonding wires to flow through the bolometer. As

shown in Figure 3.1, a capacitor and resistors in the transmission line are placed adjacent to the bolometer. This configuration allows the current induced in the bonding wires to flow through the capacitor and the current in the antenna to flow through the bolometer. The value of the resistors between the bolometer and capacitor must be large enough to prevent the current in the antenna from flowing through the capacitor. However, the addition of the resistors in the transmission line complicates the fabrication process.

Another possible low pass filter, shown in Figure 3.2, leaves out the resistors and alters the design of the bolometer. The horseshoe-shaped bolometer is actually two bolometers in parallel between the terminals of the antenna. The resistance of each bolometer is twice the resonant resistance so that the parallel combination provides the matched condition. A straightforward calculation shows that the sensitivity of the bolometer for a given current flow in the antennna is the same for either configuration.

For antennas at 230 GHz the resonant resistance is 55Ω. The series resistance of the horseshoe bolometer seen from the terminals of the transmission line is 220Ω. If the reactance of the capacitor is desired to be a factor of ten less than the series resistance of the bolometer, the value of the capacitor should be 0.2 pF or greater. With this capacitance only one tenth or less of the current induced in the transmission line will pass through the bolometer.

The design parameters for the capacitor are from Alley [2]. The finger widths and spacings are 10 μm and the length of each finger is 30 μm, as shown in Figure 4. The total length of the capacitor is kept small (110 μm) compared with the wavelength so that phase variation along the capacitor is not a problem. Without including the contribution of the ends of the fingers

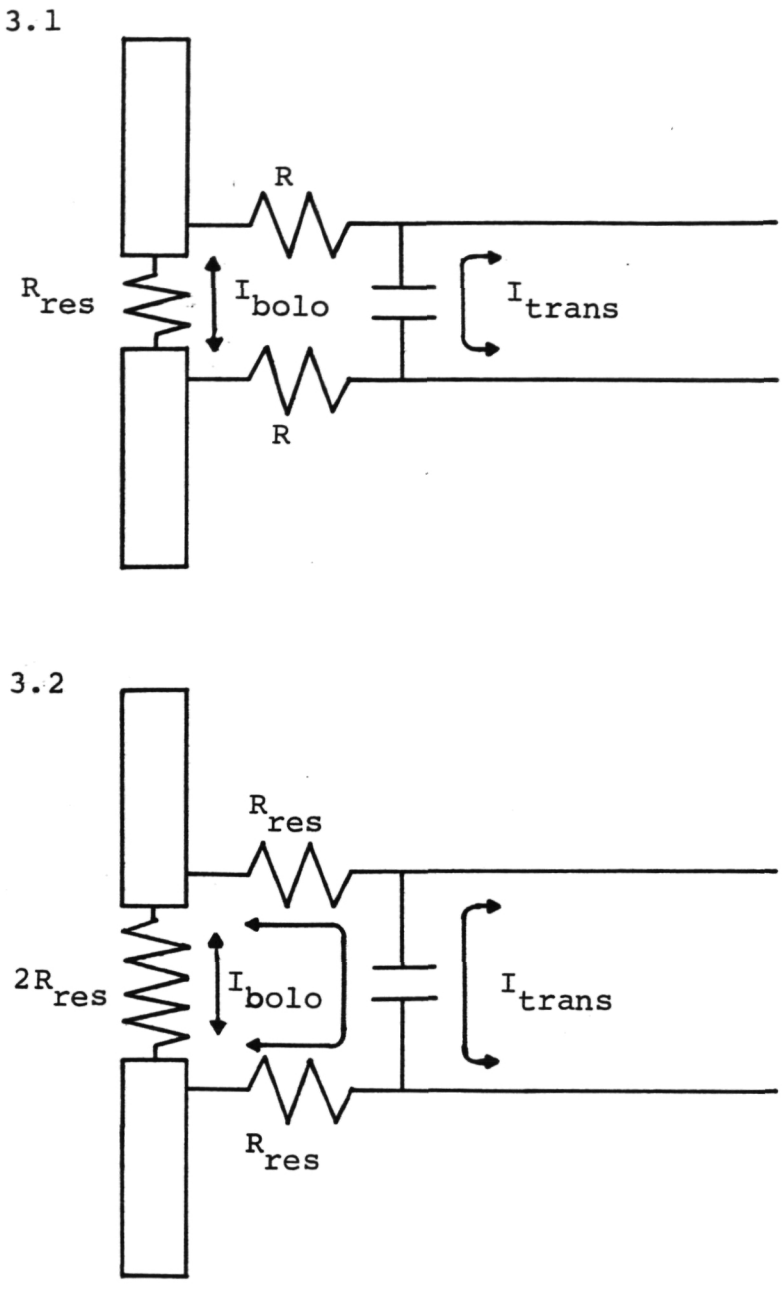

Figure 3. Two possible configurations for the low pass filter. In 3.1 the values of R and C are chosen so that current induced in the antenna flows through the bolometer and current in the bonding wires flows through the capacitor. In 3.2 the current in the bonding wires is still shorted through the capacitor, but the current in the antenna flows through two bolometers in parallel.

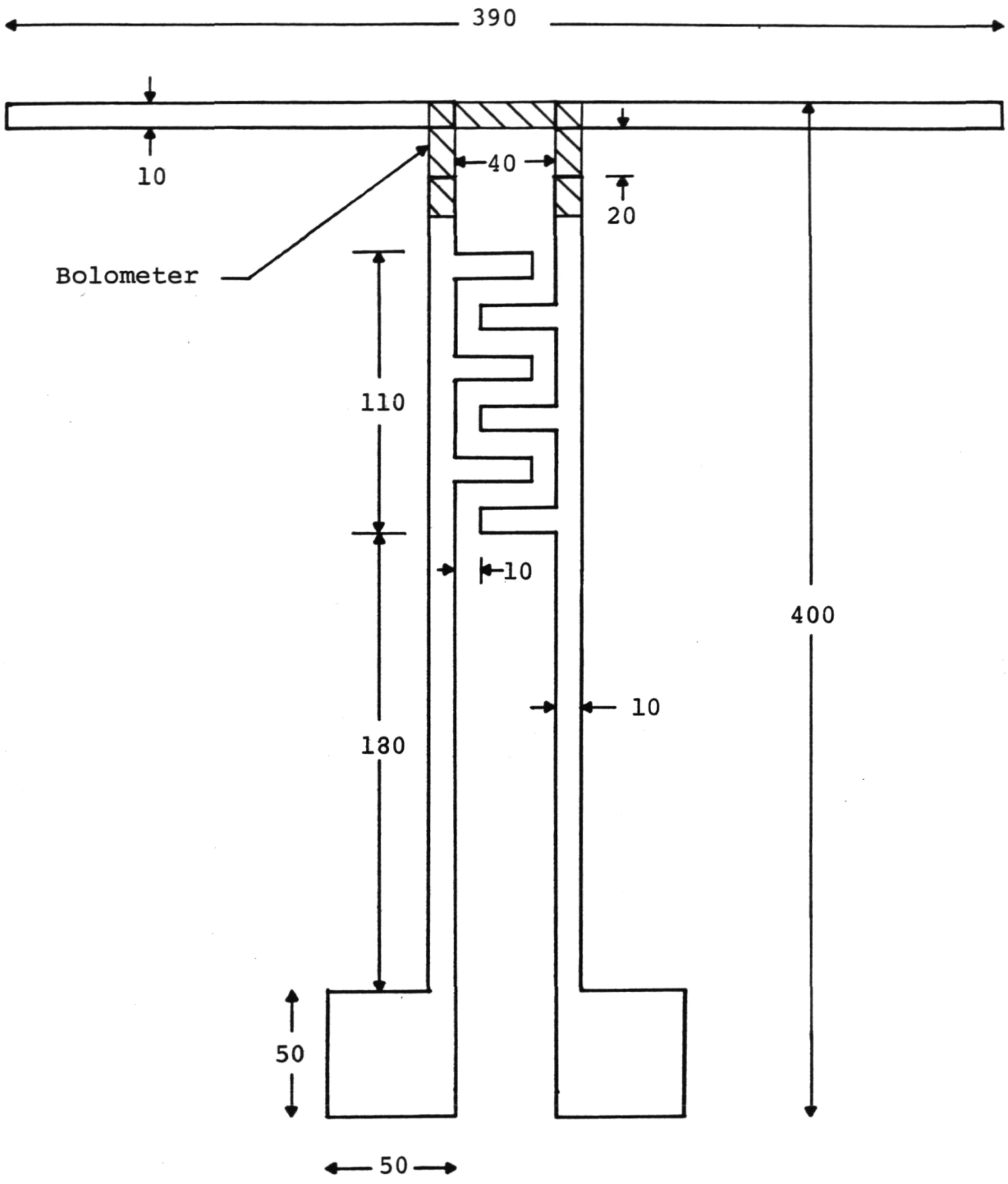

Figure 4. Diagram of new antenna design. All dimensions are in microns.

with the opposite transmission line, the capacitance is calculated to be 0.2 pF.

The remainder of the transmission line is made as long as the fly's eye camera will permit, to minimize the interaction of the bonding wires with the antenna. The bonding pads are made just large enough to bond the 1 mil gold bonding leads.

3.4 Substrate Layout

The choice of spacing the antennas on the substrate was a tradeoff between minimizing the interaction among antenna elements and fabricating enough structures to ensure several working devices. The spacing between antennas is greater than ten wavelengths. With this separation, the mutual impedence and admittance of array elements is small [3]. This allows room for eight devices on a 1.5 in. diameter substrate. Bonding islands (50 by 100 μm) are also fabricated on the substrate in order to keep the bonding wires orderly. A diagram of device placement on the substrate is shown in Figure 5.

4. FABRICATION PROCESS

The fabrication process has not been changed substantially from previous reporting periods. An outline is given below.

4.1 Photo masks

New photo masks with the refined antenna design were made. The antenna structure was cut out of rubylith at five hundred times the desired size. An IBM Model SE 401 fly's eye camera was used to make the five hundredth reduction of the rubylith cutout. The resultant photo mask has the desired structure repeated in an extended array. For this design the high resolution plate (HRP) photomask was exposed for 14 min. The development process was:

2.0 min H_2O soak

4.75 min HRP developer (5:1 dilution)

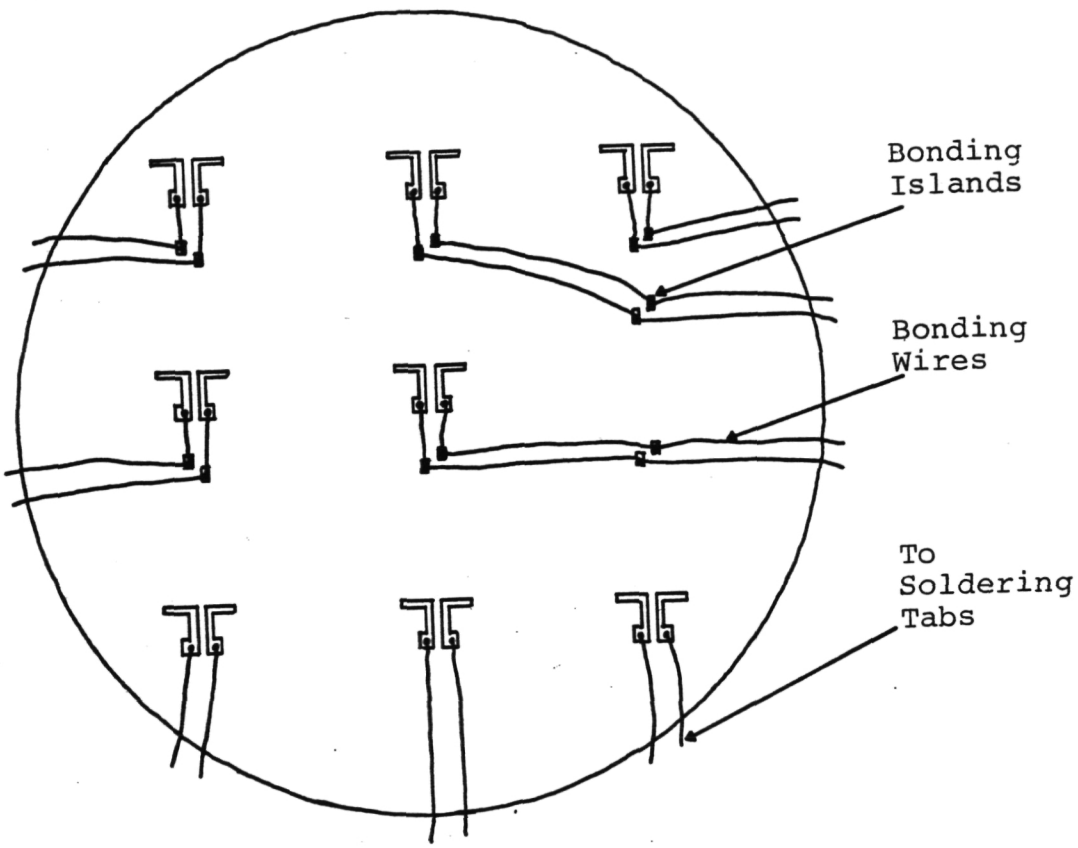

Figure 5. Layout of antennas and bonding islands on substrate. Spacing between adjacent antennas is at least ten wavelengths.

0.75 min	H_2O soak (stop bath)
1.0 min	Fixer (general fixer for films and photos)
4.0 min	H_2O soak
20 sec	50% Methanol in water
20 sec	75% Methanol in water
20 sec	Methanol

Photo masks for the antenna, bolometer and bonding islands were made. The fly's eye camera contains a multifaceted lens which causes the rubylith image to be repeated in a two dimensional grid. Many of the antenna structures formed on the photo mask were masked out with opaque tape. The end product shown in Figure 5 was obtained by repeating the selection process for the bolometer and bonding island masks.

4.2 Antenna Fabrication

The antenna fabrication process begins by cleaning the fused silica substrate. This procedure is listed below:

1) wipe substrate with cotton swab and microclean detergent;
2) rinse with distilled water for 5 min;
3) soak in hot chromic acid bath for 5 min;
4) rinse with distilled water for 5 min;
5) blow dry with nitrogen.

Next the substrate is placed in a Randex 2400 sputtering system which is then evacuated to a background pressure of less than 2 $x10^{-7}$ torr. Chromium, 125 Å, is deposited followed by gold, 4000 Å. The antennas are then etched from the Cr/Au layer. Negative photoresist (Waycoat 2:1 dilution with Waycoat thinner) is applied and then the substrate is spun at 3000 rpm for 20 sec to ensure an even coat of resist. After air drying for 30 min, the substrate is baked at 95°C for 10 min. The photo masks (antenna

masks and bonding island masks) are exposed for 10 sec each in the mask aligner. The photo resist is then developed as follows:

1) 1.0 min Waycoat developer;
2) 20 sec xylene;
3) 20 sec methanol;
4) blow dry with nitrogen;
5) bake at 110°C for 10 min.

The gold layer is then etched followed by etching of the chromium. The substrate is soaked in microstrip for 20 min to remove photoresist.

Next the positive photoresist is applied for a lift-off deposition of the bismuth bolometer. In this step a layer of photoresist is spread over the substrate. The bolometer pattern is developed in the positive resist leaving holes in the layer where the bolometers will be located. Bismuth is then deposited, adhering only to the substrate in the holes of the positive resist mask.

Hexamethyldisilazane (HMDS) is applied to the to substrate so that the positive resist will adhere to the fused silica. The substrate is air-dried for 8 min, followed by the application of positive photoresist (1350j neat). The substrate is then spun at 3000 rpm for 20 sec and baked at 95°C for 25 min. The bolometer mask is exposed for 8 sec followed by a chlorobenzene soak for 10 min which forms a lip around the holes in the photoresist resulting in better defined bolometers. The substrate is then baked at 80°C for 30 min. The photoresist is developed as follows:

1) 2/7 solution of 351 developer in water for 1 min;
2) water bath 1 min;
3) water rinse 1 min;
4) blow dry with nitrogen;
5) repeat until mask is fully developed.

The gold regions accessible through the bolometer mask are lightly etched (7 sec at half strength) to improve the gold-bismuth interface. The substrate is then placed in bismuth sputtering system which is evacuated to a background pressure of less than 2×10^{-7} torr. The bismuth is deposited using a resistance monitor to gauge the thickness. The substrate is soaked in acetone to remove excess bismuth and photoresist. Finally, the substrate is glued to the sunburst pattern of gold soldering tabs as described in an earlier report [4]. Then the bonding wires are attached from the antenna bonding pads to the intermediate bonding islands and out to the soldering tabs. The antennas are then ready for testing.

5. Experimental Procedure

Two new pieces of apparatus to facilitate precise antenna measurements were designed and built in this reporting period. One is a positioning instrument which allows the rotation of the substrate in both the theta and phi directions (spherical coordinate system) without displacement of the antenna, as shown in Figure 6. The other instrument is a mount for the Extended Interaction Oscillator (EIO) which allows changing the distance between the source and the antenna positioner without losing alignment of the incident field. Figures 7 and 8 are photographs of the antenna positioner. The first photo shows the three micrometer screws (1/4 - 40) used to place the antenna under test onto the axis of rotation of the theta positioner. The second photo shows the two translation stages used to move the desired antenna to the axis of rotation of the phi positioner. In the figures, the theta and phi rotation mounts have a black anodized coating. The phi rotation mount is set on an z-y translation stage to permit movement of the antenna and micropositioner with respect to the incident field.

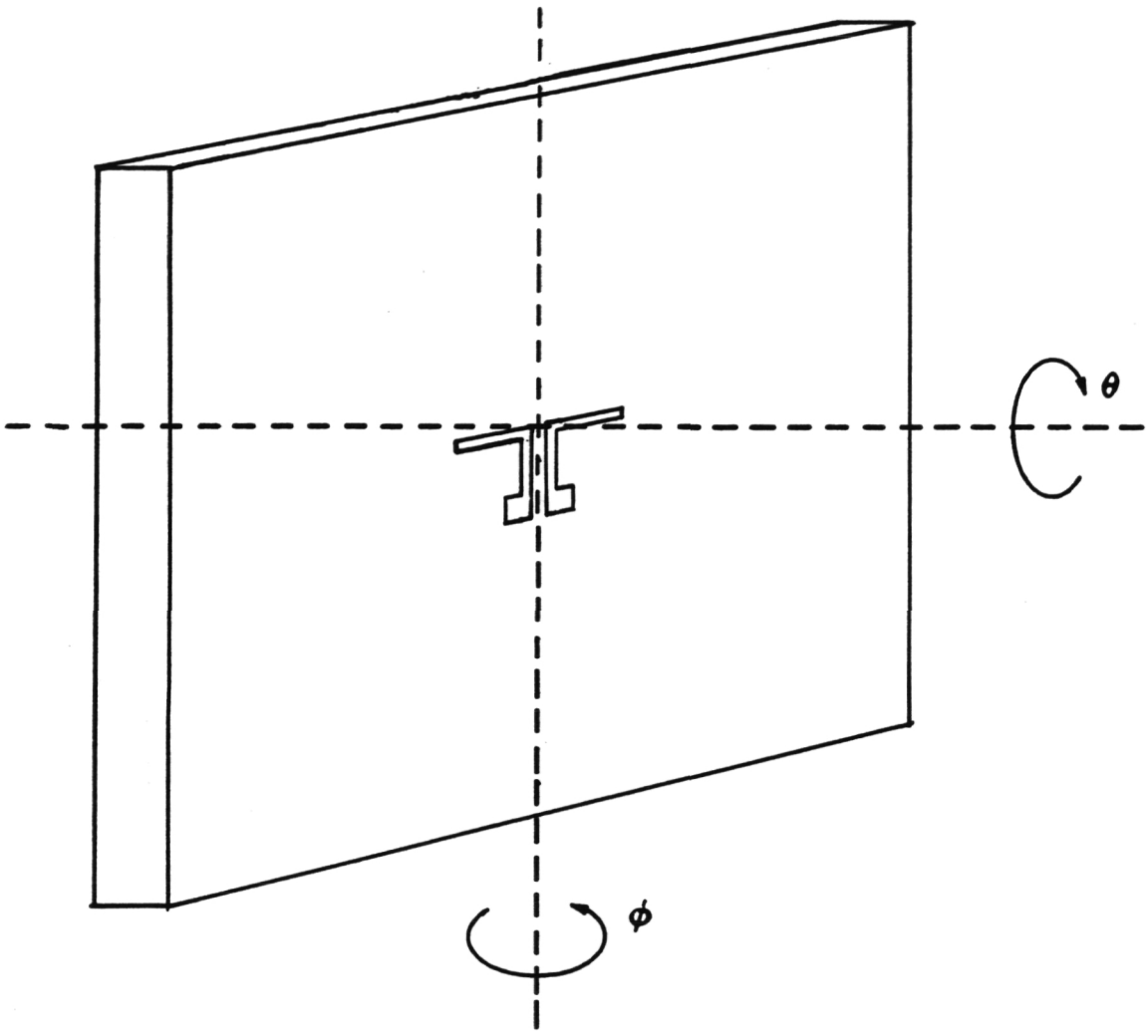

Figure 6. Illustration of the theta and phi rotation angles for antenna measurements.

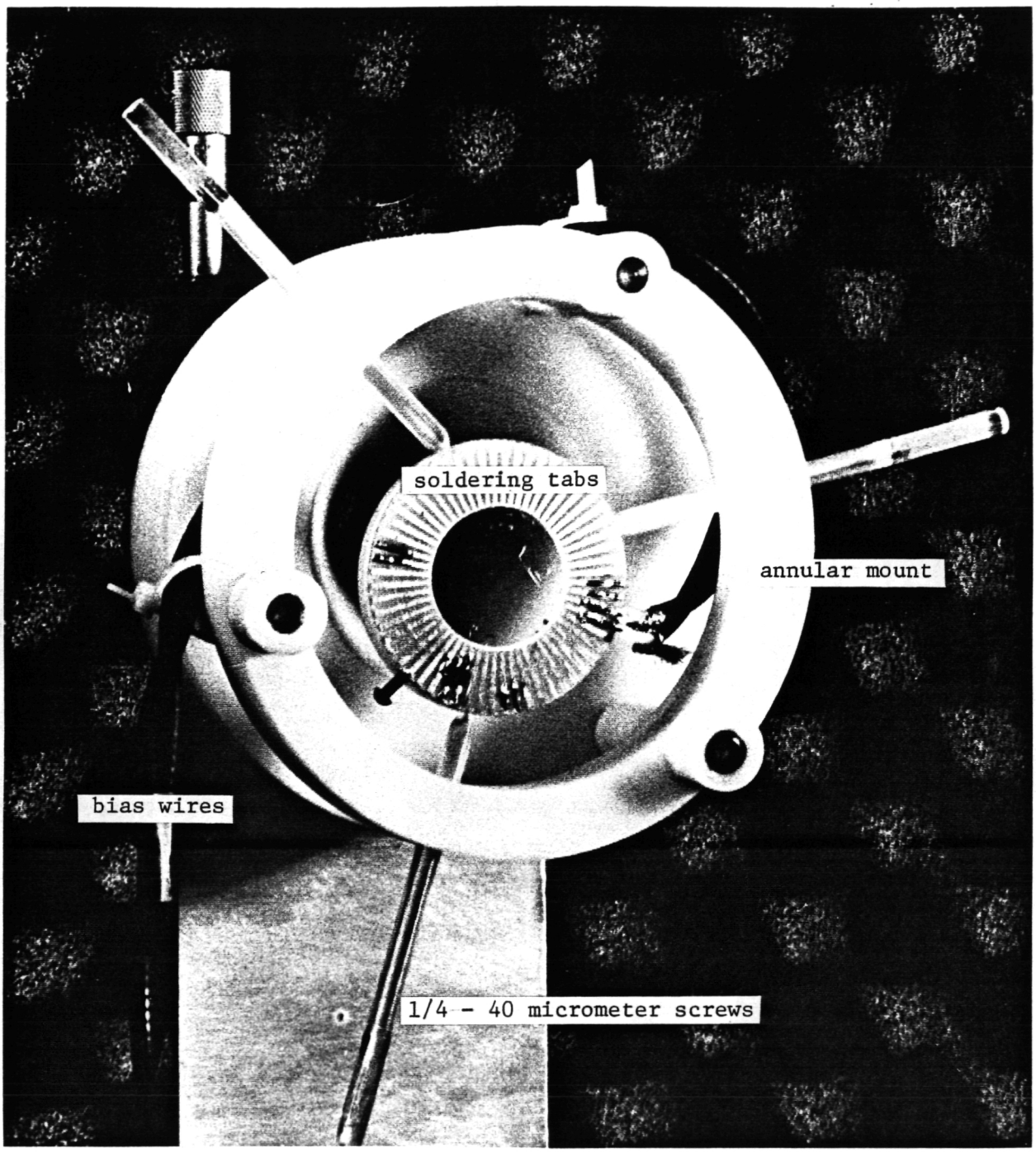

Figure 7. Photograph of positioner for the theta rotation alignment. The theta rotation device is the black mount in the rear.

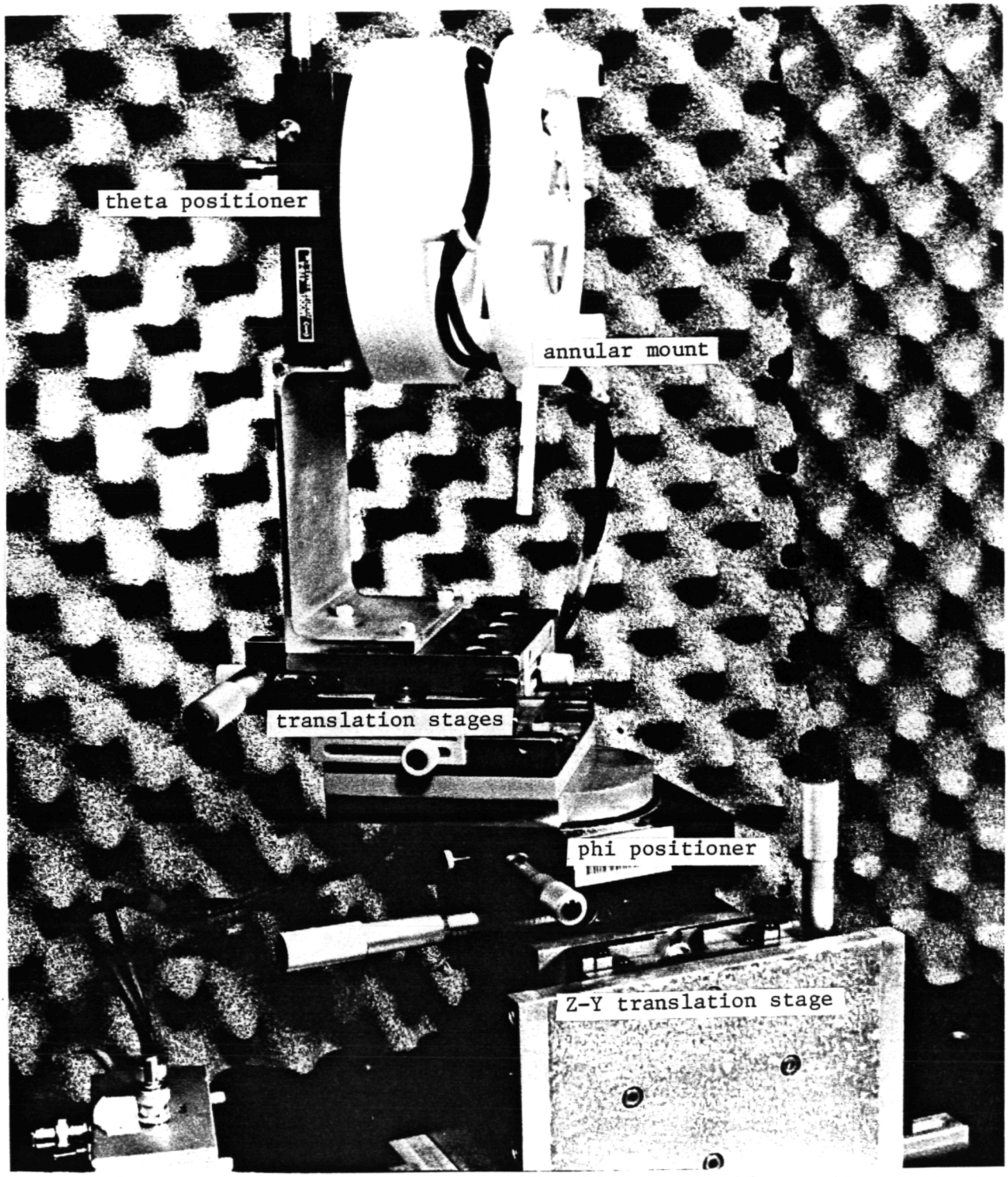

Figure 8. photograph of translation stages for phi rotation alignment. Again the black mount towards the bottom is the rotation device.

The cylindrical mount for the EIO is shown in Figure 9. A square rail is used to keep the waveguide from the EIO in alignment with the antenna positioner as the distance between the source and substrate is adjusted. Both pieces of apparatus are mounted securely to an optics table.

The complete set-up is shown in Figure 10. The chopper does not touch the optics table so that vibrations are minimal. Note the absorber which is placed around the substrate to prevent reflections of the incident field.

The alignment of the antenna in the micropositioner is made with a spotting scope containing cross hairs set up six to ten feet from the substrate. The micrometers and translation stages are adjusted until the antenna remains centered on the cross hairs under theta and phi rotations of the substrate.

The electrical connections, bias circuit and detection scheme are the same as reported in previous periods [4]. The bias circuit contains a mercury battery and precision resistors. Enough internal resistance is used in the biasing circuit to assure that a constant current is delivered to the bolometer while the antenna is under test. The biasing circuit and cables are shielded to prevent unwanted noise in the detection scheme.

The incoming radiation is mechanically chopped at 200 Hz. A lockin amplifier (IThaco 391A) is used to measure the change in voltage dropped across the bolometer when current from the incident radiation is flowing in the antenna. This change in voltage is caused by a change in resistance brought about by I^2R heat dissipation of the induced currents in the antenna. The results from tests of several antennas are given in the next section.

6. Results and Discussions

During the first part of this reporting period several

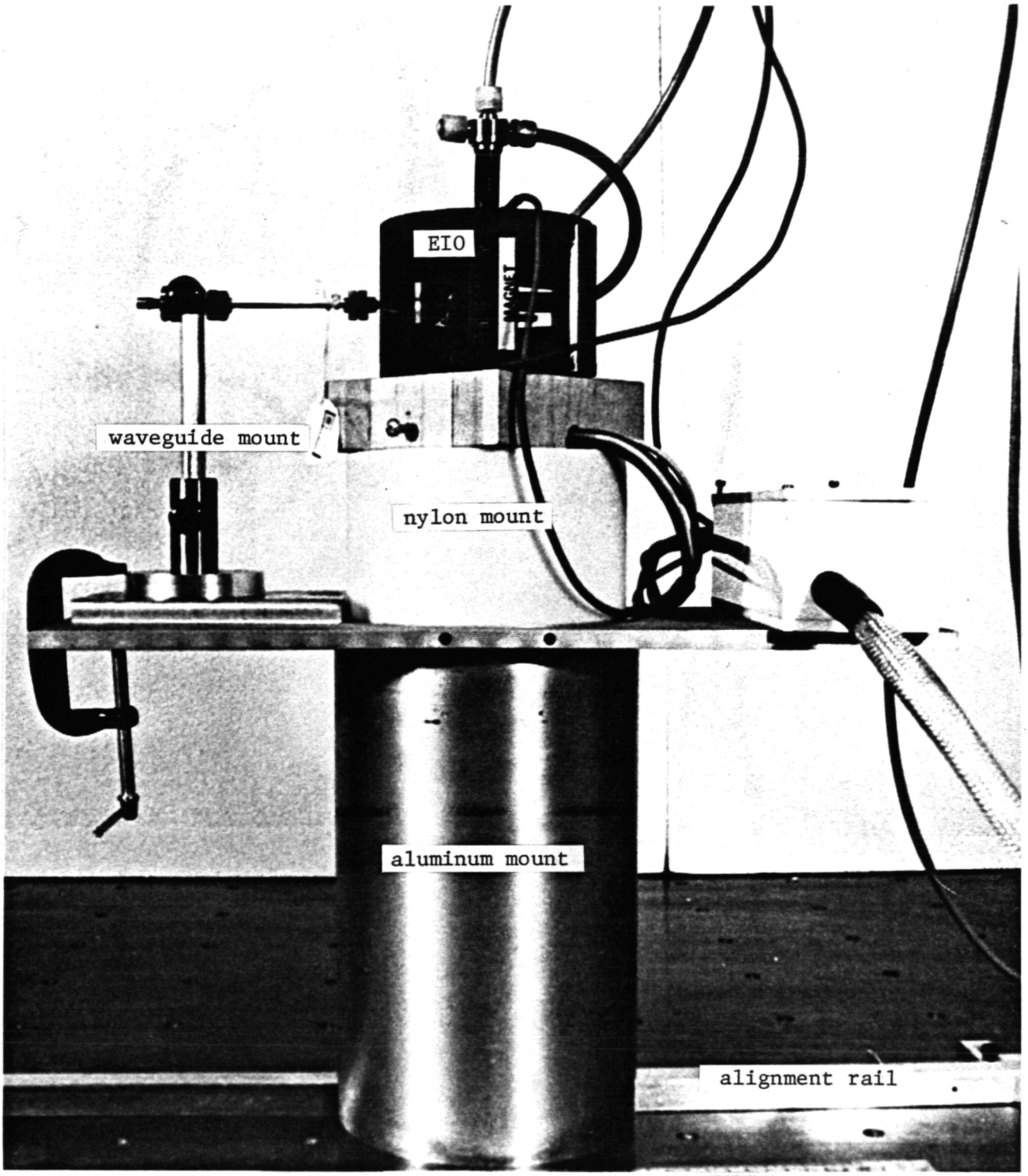

Figure 9. Photograph of cylindrical mount on a square rail for adjusting the distance between the source and substrate.

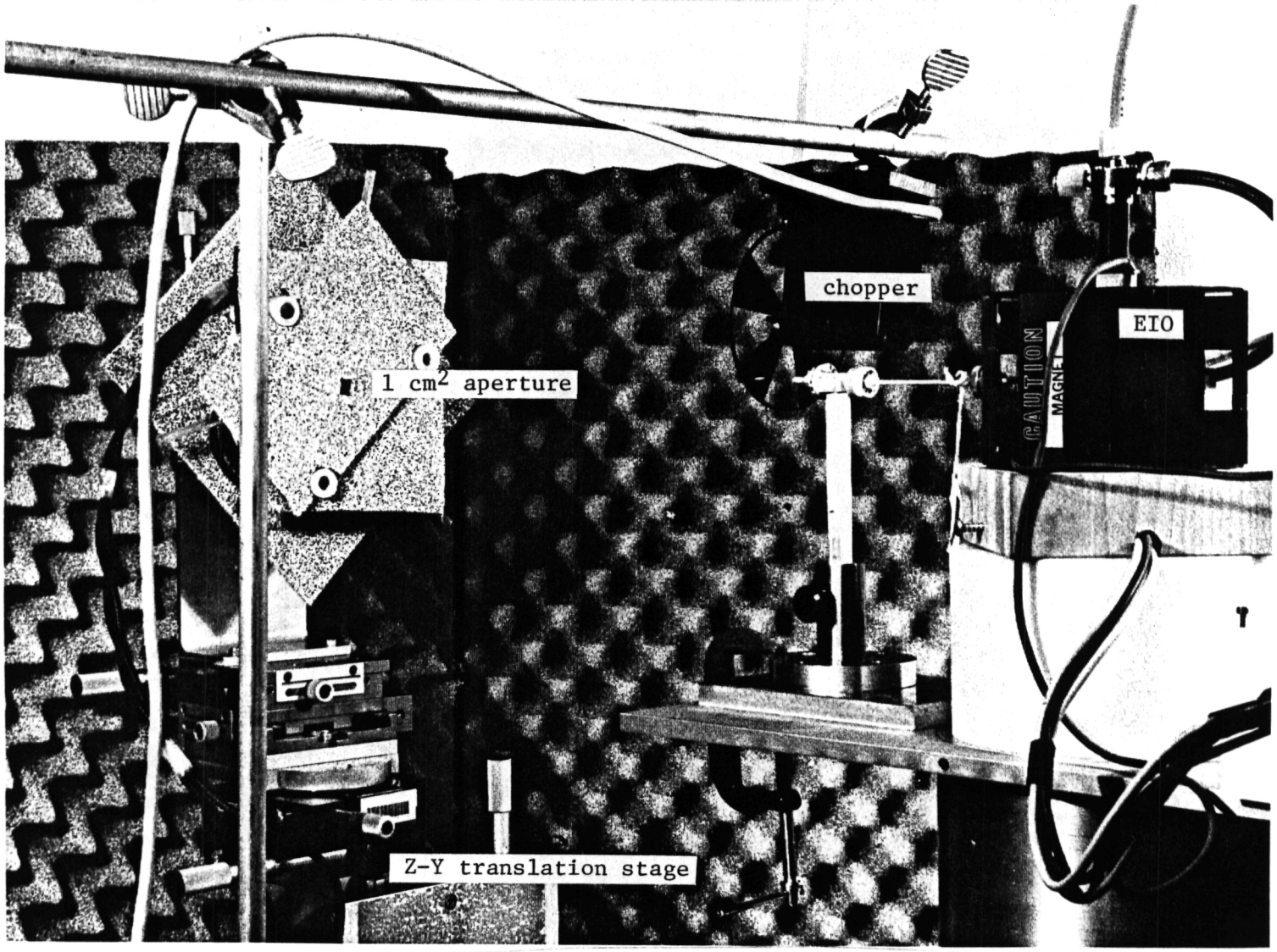

Figure 10. Photograph of complete set-up. Note the absorber around the substrate.

substrates of antennas, each with perceived refinements, were fabricated before it was concluded that the bonding wires were a major cause of distortion in the antenna behavior. In one interesting experiment worth noting, a M/A-COM beam lead diode was bonded to the transmission line of an antenna as shown in Figure 11. This structure was tested for detection of current even though the beam leads were nearly equal in length to the antenna. The diode was connected in series with a 10 Ω resistor via shielded cables. The incident beam was chopped and the voltage across the resistor was measured with a locking amplifier. A voltage of 15 μV was observed across the resistor implying that the diode was rectifing 1.5 μA of current. The percentage of radiation picked up by the bonding wires, beam leads of the diode or the antenna was not determined, but the rectified current was seen. This experiment showed the need for refinement and better understanding of the antenna structure before a quantitative statement about the rectification of current can be made.

After the new antenna design was completed, three trial fabrication runs on glass slide substrates were performed to determine the exposure and development times for the smaller geometries. The fourth and fifth fabrication runs on fused silica substrates proved fruitful, the last run showing 62 % yield. With more experience, higher yields are expected.

The results of the first antenna measurement in the new apparatus are shown as a plot in Figure 12. The axis of the dipole is rotated parallel and perpendicular to the E field component of the linearly polarized incident radiation. The theoretical curve for such a rotation (rotation about theta in Figure 6) is proportional to $\sin^2 \theta$. This measurement was carried out with no absorber around the substrate. The distortion to the pattern is caused by scattered waves from the

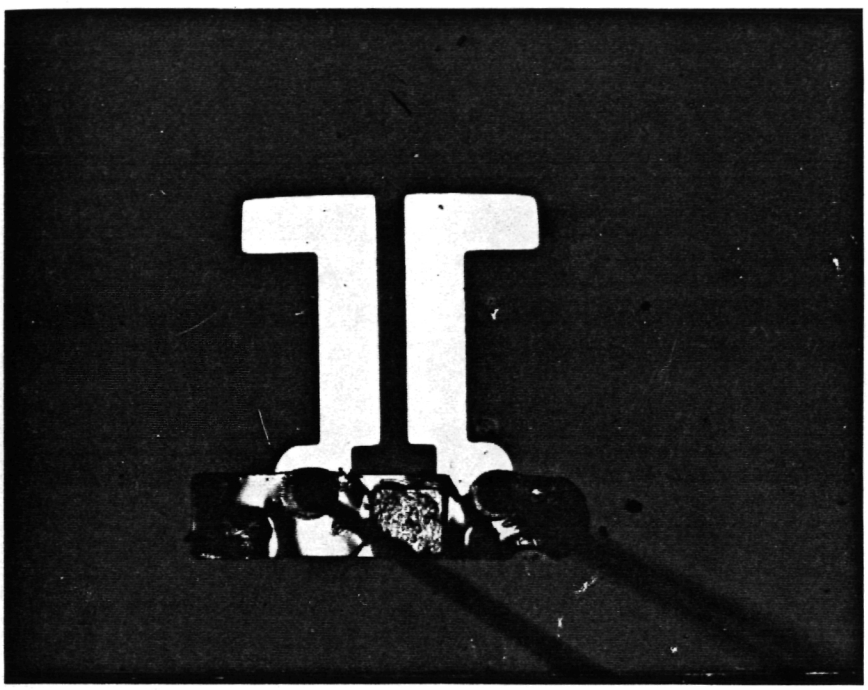

Figure 11. Photograph of the beam lead diode bonded to the old version of the antenna.

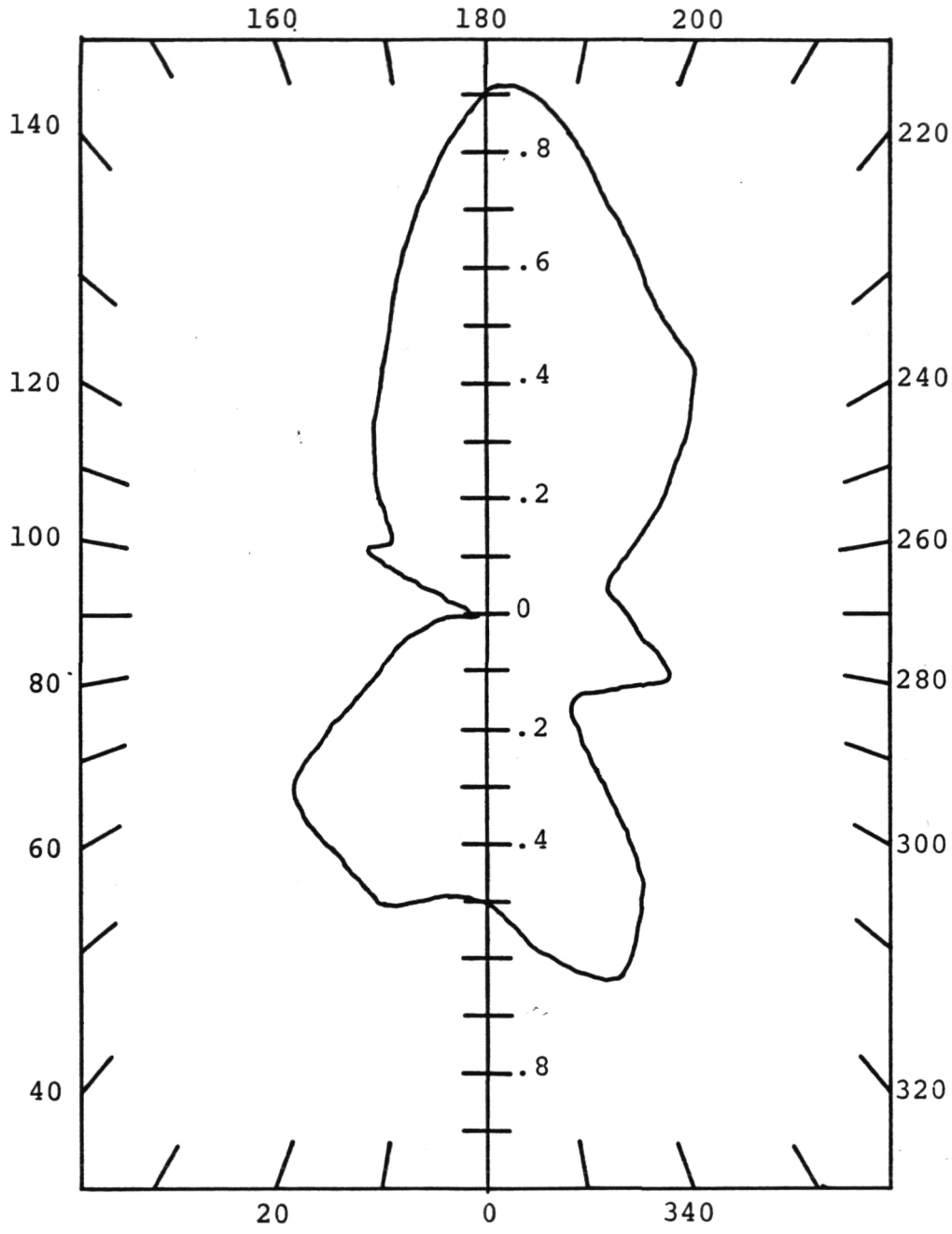

Figure 12. Plot of cross polarization measurement without absorber around antenna.

soldering tabs and bonding wires of adjacent antennas.

The measurement plotted in Figure 13 was made with an absorber placed liberally around the substrate. A sheet of absorber with a 1 cm^2 aperture was placed in front of the substrate and positioned so that only a single antenna structure and part of its bonding wires were irradiated by the incident field. The thin line in this figure is the $\sin^2\theta$ function plotted for comparison with the well established theoretical prediction.

The distortion of the lower lobe was common to all the antennas tested, and its cause has not yet been determined. The waveguide and horn antenna were checked for asymmetry by the rotation of these structures 180^o, but no change in the measured pattern was observed. Because a relatively high bias current (2-5 mA) was used, the magnetic field produced by the bias was also checked. Reversing the direction of current flow and hence the magnetic field did not alter the antenna pattern. The most likely cause is scattering from its own bonding wires. For future measurements the transmission lines will run from the antenna to the edge of the substrate and the bonding wires will be hidden under the absorber so that the effect of the transmission lines can be studied.

Figure 14 is a comparison of the measured pattern for an antenna incident directly to the radiation (14.1) with that for the substrate flipped over, (14.2). Both plots have been normalized, the measured bolometer responses were roughly equal. This is in contrast to what has been reported [5]. Reception of the radiation coming through the substrate is claimed to be significantly greater than reception to radiation incident directly on the antenna. However, all the bugs of the measurement have not been worked out as is apparent by the lobe distortion so this point will also be further investigated.

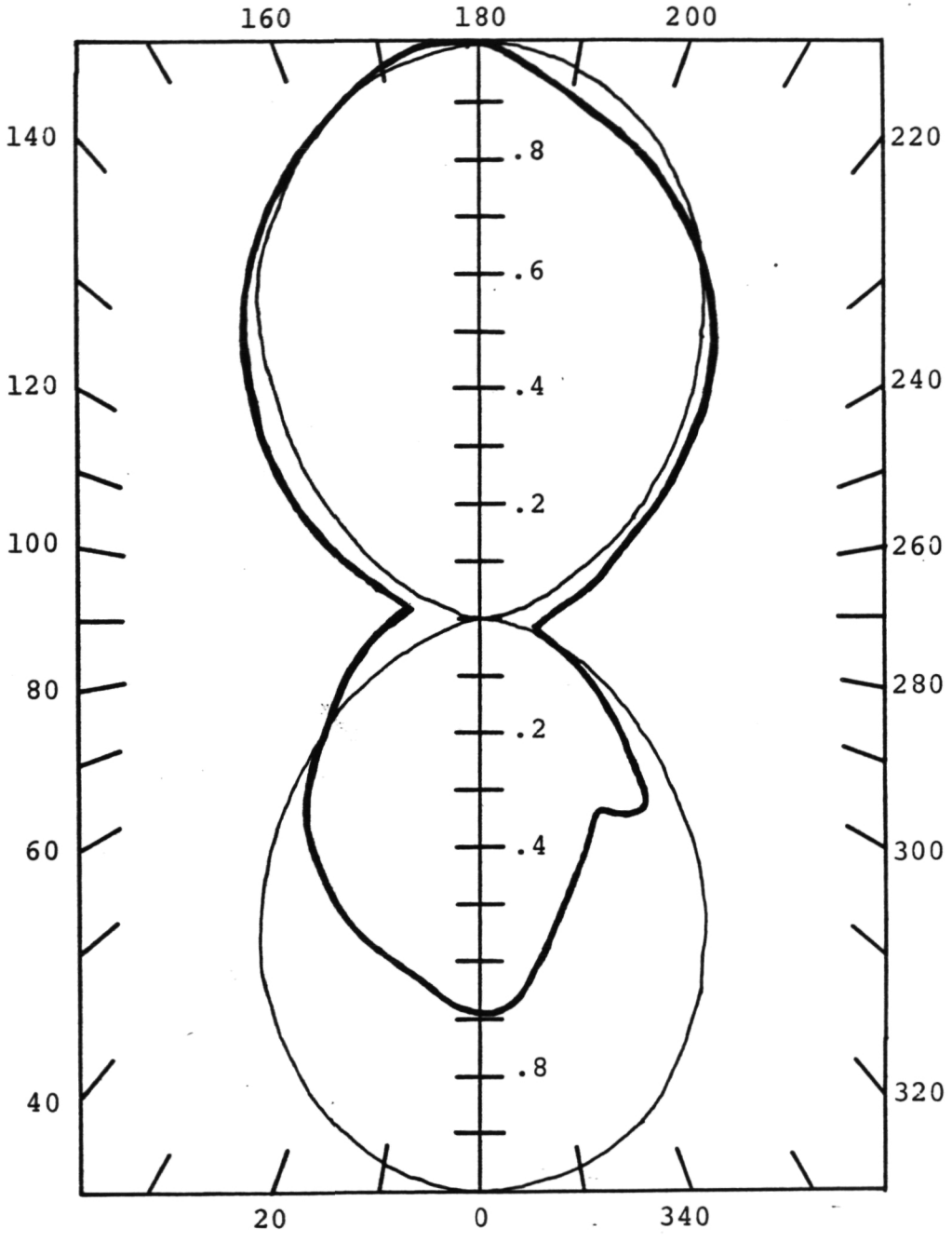

Figure 13. Plot of cross polarization measurement with absorber. The thin line is the theoretical prediction for this measurement.

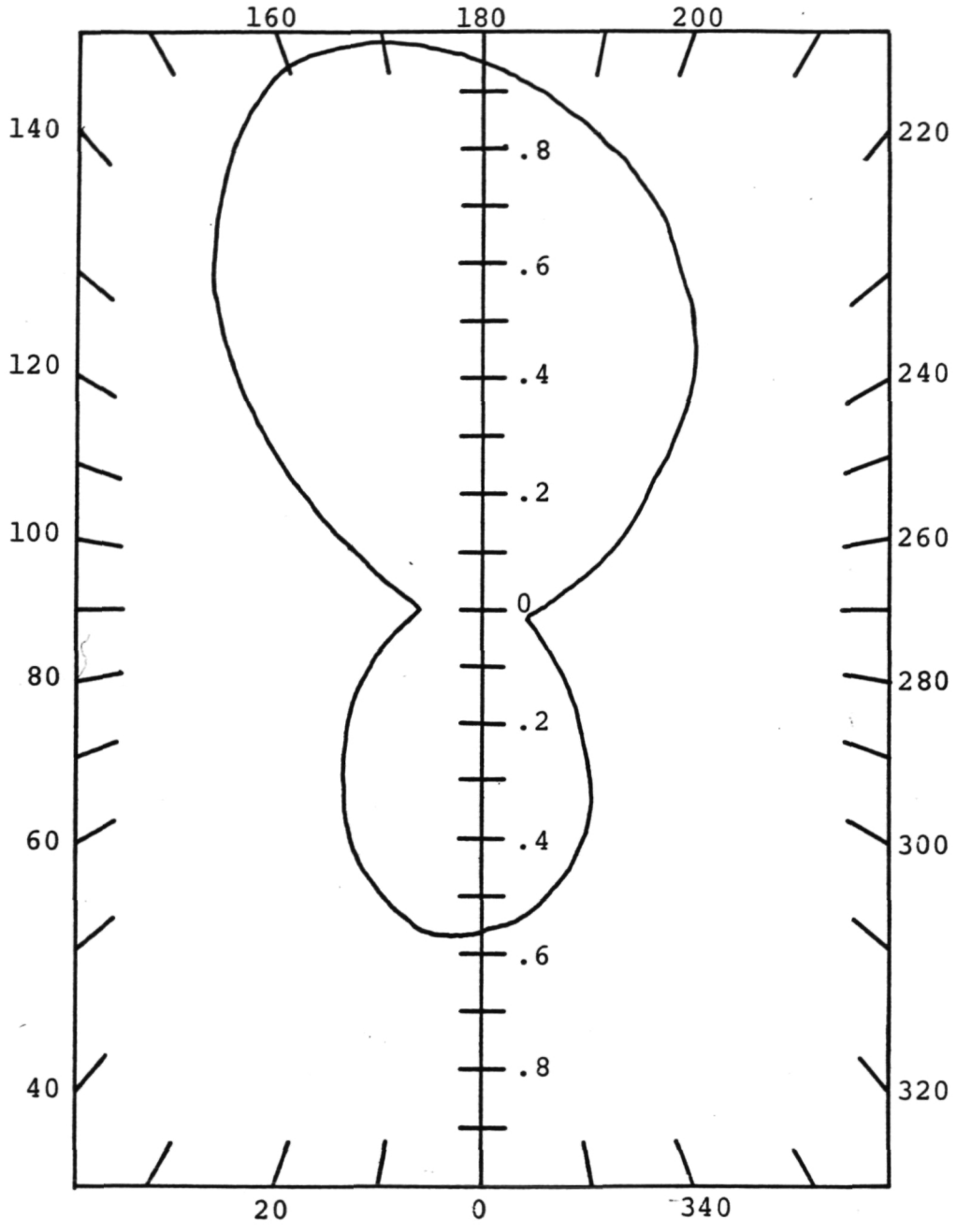

Figure 14.1 Comparison of the response of the antenna structure for radiation incident directly on the antenna, shown above, and radiation incident on the antenna through the substrate shown in figure 14.2.

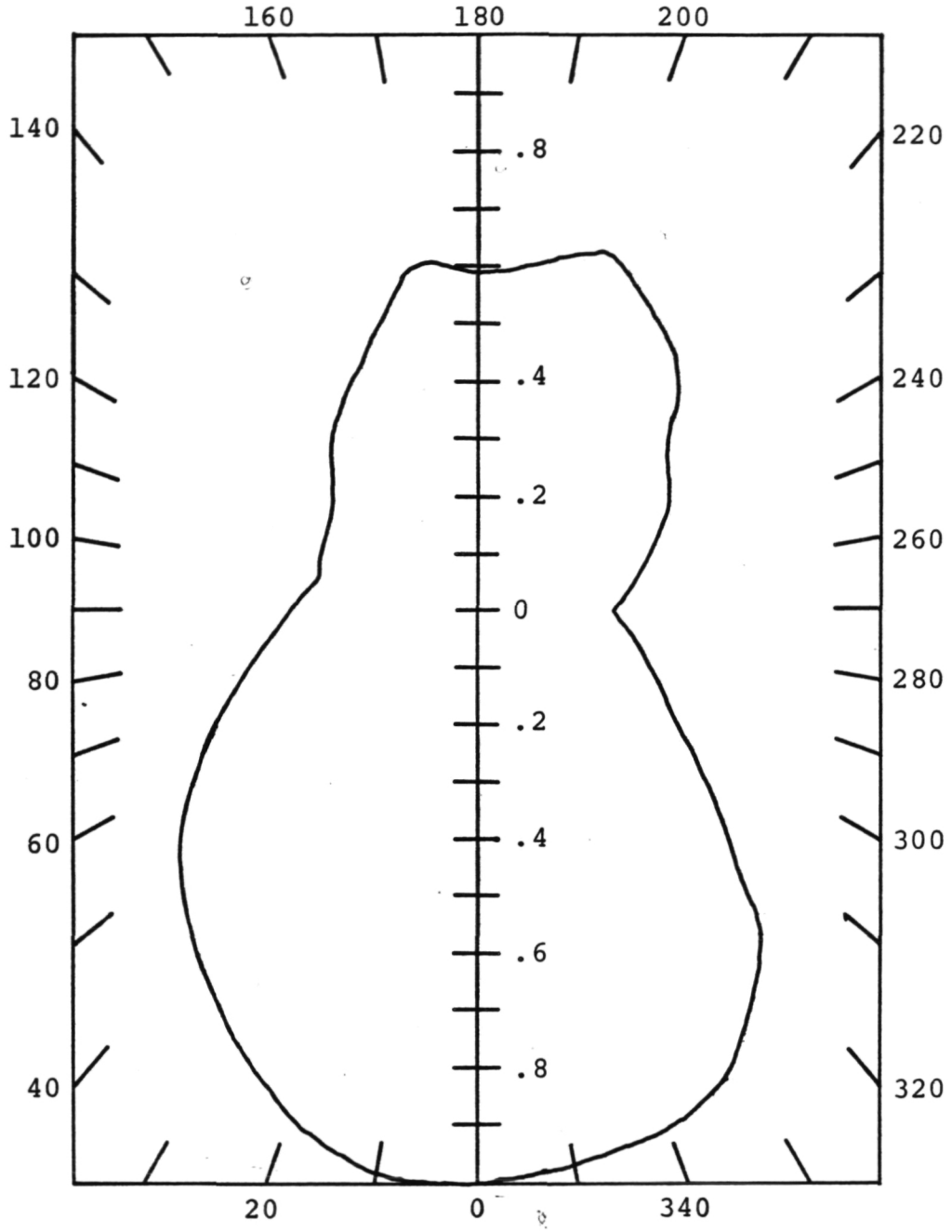

Figure 14.2 Response of the antenna structure for radiation incident through the substrate.

7. Conclusions and Future Work

The understanding of the antenna aspects of the rectenna problem has greatly increased in this reporting period. The addition of a low pass filter and refinement in the measurement apparatus have facilatated confirmation of the dipole pattern of the antenna. The antenna structure has been redesigned utilizing 10 m geometries. The horseshoe shaped bolometer and interdigitated capacitor have increased the level of sophistication in the devices. There are still a few problems to resolve with the transmission line, but this work should proceed quickly. The major effort for the next reporting period will be the development and integration of a MOM diode into the antenna structure. The first step in this process will be the construction and testing of the diode by itself. Then the diode will be placed in the rectenna using a matching transmission line.

Work has begun on the development of the diode structure. The first generation is a three step process patterned after the work of Heiblum et al. [6]. In this design the cross section area of the diode is kept small by using the edge, not the top, of the oxide region for the metal-oxide interface. This approach minimizes the diode contact area without increasing the complexity of the fabrication process.

The diode structure is shown in Figure 15. The first metallization is a chromium/gold layer to provide nonoxiziding contacts for testing purposes. A nickel layer followed by a silicon dixiode layer is deposited over the chromium/gold contacts. A 20 x 40 μm island centered on the edge of one contact is formed from this layer. The nickel at the base of the island is the first half of the diode. Next the substrate is placed in the sputtering unit and back sputtered (or sputter

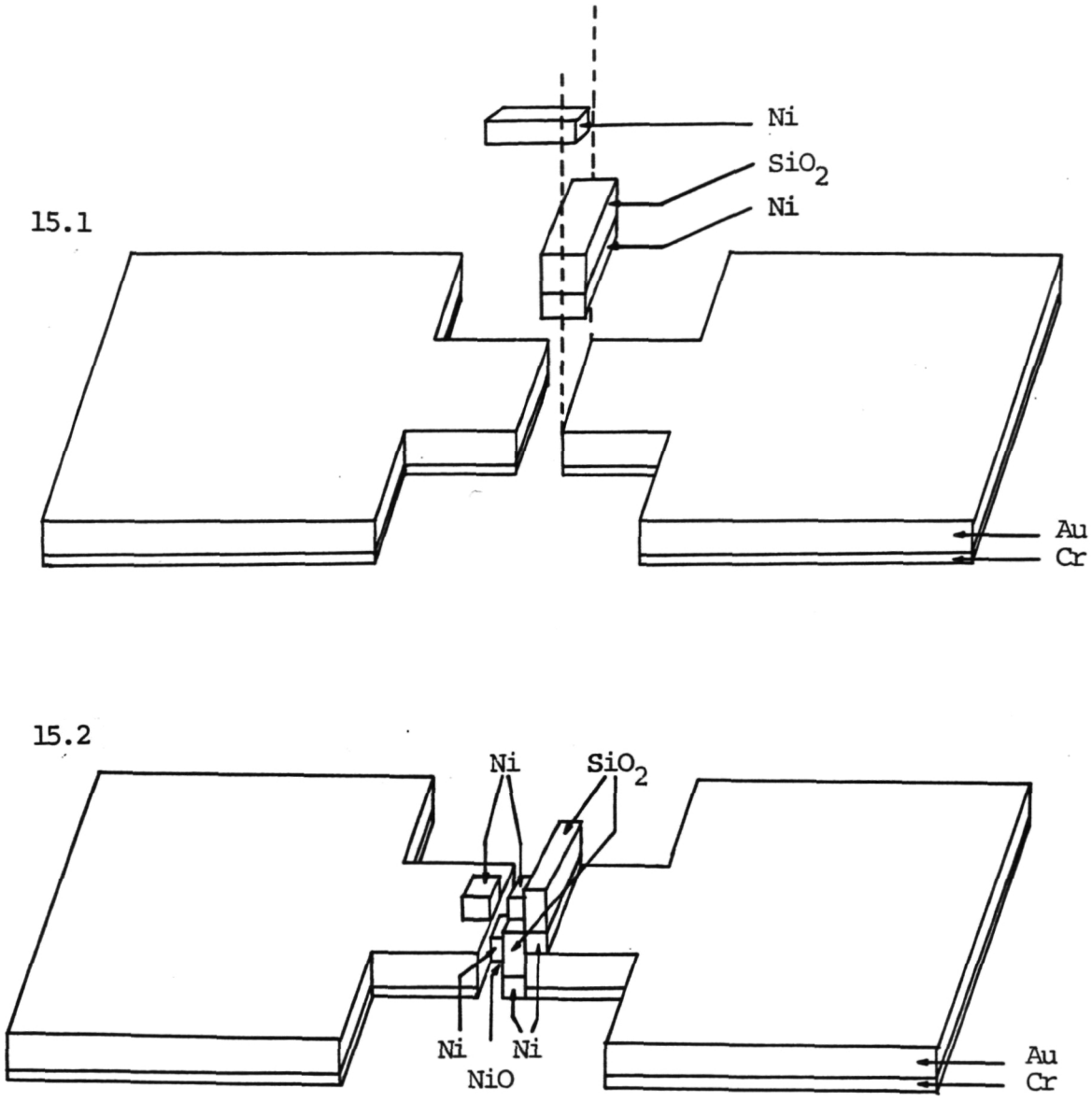

Figure 15. 1. Illustration of three layer fabrication of MOM diode. 2. Drawing of completed diode. Note the oxide layer is found in the edge of the first nickel metalization.

etched) to remove the oxide layer which forms spontaneously in the atmosphere on the exposed nickel surface. A layer of oxide on the edge of the nickel metalization is grown while the substrate is still in the sputtering unit [6]. The final layer of nickel (or some other metal for a non-symetric diode) is deposited. The last section of the diode is etched from this layer.

The integration with the antenna will be undertaken after the diode structure has been fabricated and characterized. The characteristic impedance of the transmission line will have to be calculated to determine proper placement of the diode. The schematic of the rectenna design is shown in figure 16. The resistors are added between the diode and the capacitor to prevent the current in the antenna from flowing through the capacitor.

In summary, the work performed in this reporting period has confirmed the dipole behavior of the antenna structure. Fabrication expertise has increased with the utilization of 10 μm geometries and implementation of the interdigitated capacitor. Work has begun on the MOM diode, and an integrated rectenna will be fabricated in the next reporting period. After successful demonstration of rectenna action at millimeter wave frequencies, the effort will shift to fabrication of a device for operation in the infrared region.

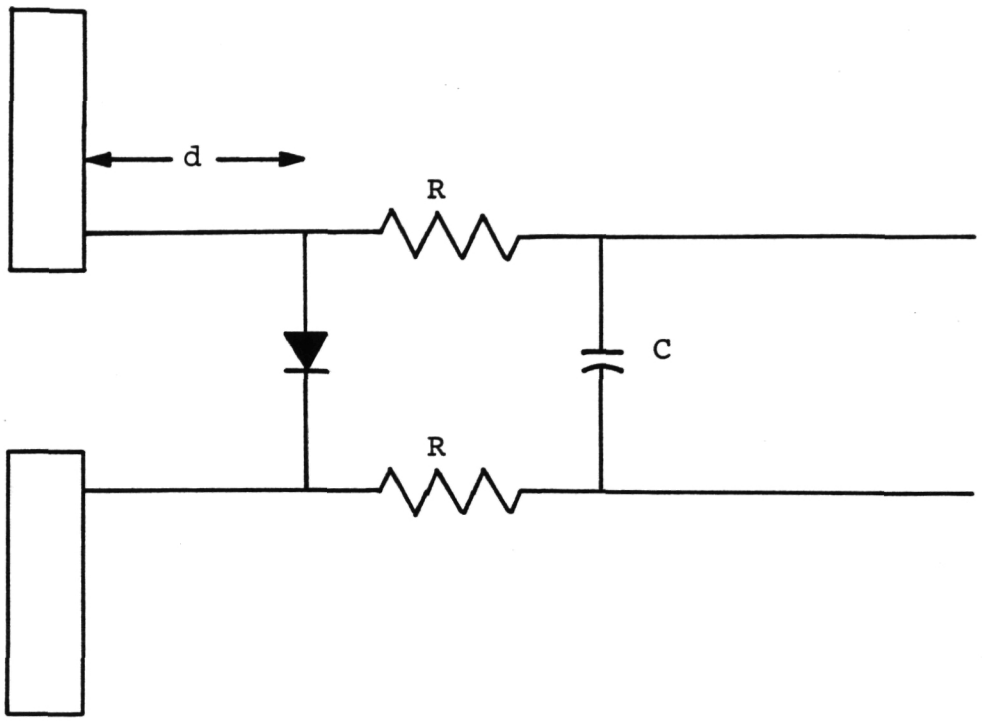

Figure 16. Schematic for the rectenna devices. Resistors are added in the low pass filter to prevent the current in the antenna from flowing through the capacitor.

References

1. M. Kominami, D. M. Pozar and D. H. Schaubert, "Dipole and Slot Elements and Arrays on Semi-Infinite Substrates," IEEE Trans. Ant. and Prop., vol. AP-33, pg. 600-607, June 1985.

2. G. D. Alley, "Interdigital Capacitors and Their Application to Lumped-Element Microwave Integrated Circuits," IEEE Trans. Microwave Theory and Tech., vol. MTT-18, pg. 1028-1033, December, 1970.

3. C. A. Balanis, Antenna Theory, pg. 296 - 307, Harper and Row, New York, NY, 1082.

4. D. P. Campbell, M.A. Gouker and J. J. Gallagher, "Semi-Annual Status Report on Infrared Technology for Satellite Power Conversion," December 11, 1984.

5. D. B. Rutledge, D. P. Neikirk and Kasiligam, in "Infared and Millimeter Waves", vol. 10 (K. J. Guton, ed.) pg 9., 1983.

6. M. Heiblum, S. Wang, J. R. Whinnery, an T. K. Gustafon, "Characteristics of Integrated MOM Junctions at dc and at Optical Frequencies," IEEE J. of Quant. Elec, vol. QE-14, pg. 159 - 169.